Cellular Microbiology (2009) doi:10.1111/j.1462-5822.2009.01396.x

The *Pseudomonas syringae* type III effector HopG1 targets mitochondria, alters plant development and suppresses plant innate immunity

Anna Block,[1,2] Ming Guo,[1,2] Guangyong Li,[1,2] Christian Elowsky,[3] Thomas E. Clemente[1,3] and James R. Alfano[1,2]*

[1]*The Center for Plant Science Innovation, University of Nebraska, Lincoln, Nebraska, USA.*
[2]*Department of Plant Pathology, University of Nebraska, Lincoln, Nebraska, USA.*
[3]*Center for Biotechnology, University of Nebraska, Lincoln, Nebraska, USA.*

Summary

The bacterial plant pathogen *Pseudomonas syringae* uses a type III protein secretion system to inject type III effectors into plant cells. Primary targets of these effectors appear to be effector-triggered immunity (ETI) and pathogen-associated molecular pattern (PAMP)-triggered immunity (PTI). The type III effector HopG1 is a suppressor of ETI that is broadly conserved in bacterial plant pathogens. Here we show that HopG1 from *P. syringae* pv. *tomato* DC3000 also suppresses PTI. Interestingly, HopG1 localizes to plant mitochondria, suggesting that its suppression of innate immunity may be linked to a perturbation of mitochondrial function. While HopG1 possesses no obvious mitochondrial signal peptide, its N-terminal two-thirds was sufficient for mitochondrial localization. A HopG1–GFP fusion lacking HopG1's N-terminal 13 amino acids was not localized to the mitochondria reflecting the importance of the N-terminus for targeting. Constitutive expression of HopG1 in *Arabidopsis thaliana*, *Nicotiana tabacum* (tobacco) and *Lycopersicon esculentum* (tomato) dramatically alters plant development resulting in dwarfism, increased branching and infertility. Constitutive expression of HopG1 *in planta* leads to reduced respiration rates and an increased basal level of reactive oxygen species. These findings suggest that HopG1's target is mitochondrial and that effector/target interaction promotes disease by disrupting mitochondrial functions.

Introduction

Many Gram-negative phytopathogenic bacteria use a syringe-like apparatus called a type III secretion system (T3SS) to inject type III effector (T3E) proteins into plant cells to promote pathogenicity (Alfano and Collmer, 2004). The T3SS of the hemibiotrophic pathogen *Pseudomonas syringae* is encoded by the *hrp* and *hrc* genes located within the Hrp pathogenicity island and is often referred to as the Hrp T3SS (Alfano *et al.*, 2000). *P. syringae* pv. *tomato* DC3000 has become an important model pathogen as it infects both *Lycopersicon esculentum* (tomato) and the model plant *Arabidopsis thaliana* in a T3SS-dependent manner. Bioinformatic analysis of the DC3000 genome has lead to the identification of over 30 T3Es most of whose activities and plant targets remain unknown (Lindeberg *et al.*, 2006). DC3000 mutants defective in their T3SS are non-pathogenic reflecting the requirement of the T3Es for pathogenicity. However, pathogenesis of DC3000 mutants defective in individual T3Es is in general only slightly compromised, suggesting that many T3Es are functionally redundant. More recently, it was discovered that a primary target for many *P. syringae* T3Es is the plant innate immune system (Espinosa and Alfano, 2004; Abramovitch *et al.*, 2006).

The plant innate immune system is composed of at least two branches (Jones and Dangl, 2006). First, extracellular plant receptors recognize conserved molecules on microorganisms called pathogen-associated molecular patterns (PAMPs) sometimes referred to as microbe-associated molecular patterns (MAMPs), which are present on pathogenic and non-pathogenic microbes (Nurnberger *et al.*, 2004; Ausubel, 2005). PAMP recognition activates plant innate immune responses that are collectively referred to as PAMP-triggered immunity (PTI). Several plant pathogen T3Es have been shown to suppress outputs of PTI (Alfano and Collmer, 2004; Chisholm *et al.*, 2006). Plants likely evolved the second branch of

Received 17 June, 2009; revised 25 September, 2009; accepted 10 October, 2009. *For correspondence. E-mail jalfano2@unl.edu; Tel. (+1) 402 472 0395; Fax (+1) 402 472 3139.

the plant innate immune system, referred to as effector-triggered immunity (ETI) (Jones and Dangl, 2006), to counter the ability of pathogen effectors to suppress PTI. ETI is based on the ability of resistance (R) proteins to recognize pathogen effectors resulting in the activation of innate immune pathways. There is overlap between the outputs of PTI and ETI (Tao *et al*., 2003; Zipfel *et al*., 2004; Tsuda *et al*., 2008). However, ETI is generally considered a more substantial immune response that usually includes the hypersensitive response (HR), a form of programmed cell death (PCD) elicited on microbial attack. Bacterial plant pathogen T3Es have also been shown to suppress ETI (Jamir *et al*., 2004; Abramovitch *et al*., 2003). The fact that some T3Es seem capable of suppressing both PTI and ETI suggests that these T3Es have multiple targets or that they are targeting shared components of PTI and ETI.

While the activities and targets for most plant pathogen T3Es remain unknown, there has been recent progress made for several *P. syringae* T3Es (Block *et al*., 2008; Zhou and Chai, 2008; Cunnac *et al*., 2009). Insight into the role that T3Es are playing in pathogenesis can be gained by elucidating their subcellular localization. For example, several *P. syringae* T3Es possess myristoylation sites, suggestive of membrane targeting. These include AvrRpm1 (Nimchuk *et al*., 2000), AvrB (Nimchuk *et al*., 2000), AvrPto (Shan *et al*., 2000), AvrPphB (Nimchuk *et al*., 2000), HopF2 (Robert-Seilaniantz *et al*., 2006) and HopZ1 (Lewis *et al*., 2008). Mutation of the myristoylation sites within these T3Es abolishes their function. The AvrBs3 T3E family from phytopathogenic species of *Xanthomonas* are targeted to the nucleus where they act as transcription factors (Yang and Gabriel, 1995; Van den Ackerveken *et al*., 1996; Yang *et al*., 2000). To date, the only T3E demonstrated to localize to plant organelles is HopI1 from *P. syringae*, which targets and remodels chloroplasts (Jelenska *et al*., 2007).

We have previously demonstrated that several DC3000 T3Es, including HopG1, are suppressors of ETI responses including the HR (Jamir *et al*., 2004). HopG1 was originally identified in a genome-wide screen for T3Es and was confirmed to be secreted in culture by DC3000 (Petnicki-Ocwieja *et al*., 2002). The expression of HopG1 in yeast or tobacco can suppress cell death triggered by the pro-apoptotic mouse protein Bax (Jamir *et al*., 2004), which is consistent with HopG1 acting as an ETI suppressor. Additionally, HopG1 was shown to be capable of suppressing vascular restriction in infected leaves (Oh and Collmer, 2005).

Communicated herein are additional functional analyses on HopG1 that provide insight on how it suppresses PCD and other innate immune responses. We demonstrate that *hopG1* is expressed in conditions that induce type III secretion and that a HopG1 protein fusion is injected into plant cells in a type III dependent manner. We show that HopG1 is capable of suppressing PTI as well as ETI responses. Importantly, we show that HopG1 localizes to plant mitochondria, suggesting that its targets in this organelle are involved in both PTI and ETI. Surprisingly, the constitutive expression of HopG1 *in planta* causes altered plant morphology and infertility possibly due to disruption of normal mitochondrial function by HopG1. We found that transgenic *A. thaliana* plants expressing HopG1 had reduced rates of respiration and enhanced basal levels of reactive oxygen species, further implying that mitochondrial function in these plants is impaired. Taken together, these data suggest a broadly conserved pathogenic strategy where HopG1 suppresses host innate immunity by disrupting mitochondrial functions.

Results

HopG1 is a conserved protein found in several clades of bacteria

T3Es with high similarity to HopG1 are found in several T3SS-containing phytobacteria (Fig. S1). The per cent protein identities as determined by pairwise BLAST of HopG1 from DC3000 with proteins that share similarity to HopG1 are as follows: *P. syringae* pv. *phaseolicola* 1448 A (53%); *Ralstonia solanacearum* GMI1000 (52%); *Xanthomonas axonopodis* pv. *citri* (46%); *X. campestris* pv. *campestris* ATCC 33913 (48%); *Acidovorax avenae* ssp. *citrulli* AAC00-1 (46%) and *Rhizobium etli* CFN 42 (46%). We identified a putative cyclophilin binding site motif (GPxL) in the C-terminal half of these proteins (Fig. S1). This motif is found in the *P. syringae* T3E AvrRpt2, where it was shown to be necessary for the binding of a *A. thaliana* cyclophilin, a prerequisite for the proper folding and activity of AvrRpt2 (Coaker *et al*., 2006). Bioinformatic analyses of HopG1's peptide sequence did not reveal additional insights as to its function or cellular target(s). However, the evolutionary conservation of HopG1-like T3Es across a range of plant-associated bacteria suggests that they have an important function in different types of bacterial–plant interactions.

DC3000 hopG1 *expression is enhanced in type III-inducing conditions and HopG1 is injected into plant cells*

Bioinformatic analysis of DC3000 identified a putative Hrp box upstream of *hopG1*. Hrp boxes are binding sites for the alternative sigma factor HrpL that regulates the expression of genes under T3SS-inducing conditions (Xiao and Hutcheson, 1994). To experimentally demonstrate if *hopG1* is expressed under T3SS-inducing

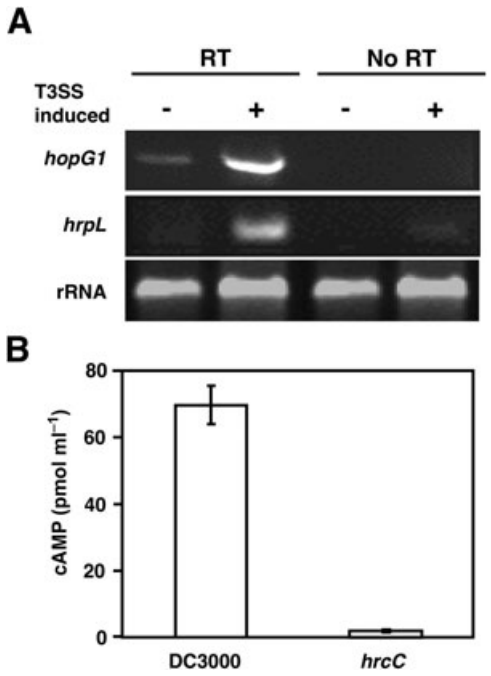

Fig. 1. *hopG1* is expressed in T3SS-inducing conditions and translocated into plant cells via the T3SS.
A. Semi-quantitative RT-PCR of *hopG1* and *hrpL* from DC3000 grown for 3 h in rich media (–) or in T3SS-inducing minimal media (+). *hopG1* and *hrpL* were expressed at higher levels in T3SS-inducing medium than in rich media, indicating that *hopG1* is induced with the T3SS.
B. Adenylate cyclase (CyaA) translocation assay of C-terminal CyaA fusions of HopG1 constitutively expressed in wild-type DC3000 and the T3SS deficient DC3000 *hrcC* mutant. The cAMP level indicates the amount of protein injected into plant tissues (the standard errors are indicated, $P < 0.001$). Each experiment was repeated at least twice with similar results.

conditions, we isolated DC3000 RNA from cultures grown under T3SS-inducing and non-inducing conditions and performed semi-quantitative RT-PCR. These experiments showed that *hopG1* expression was increased in T3SS-inducing conditions in a manner similar to *hrpL* (Fig. 1A).

To determine if HopG1 is translocated into plant cells by the T3SS we used an adenylate cyclase (CyaA) fusion assay (Sory *et al.*, 1995). This assay determines if a protein can be injected into the plant cell as CyaA is dependent on calmodulin for its activity, and produces measurable levels of cAMP only when it is inside the plant cell but not when it is in the bacterial cell or plant apoplast. The presence of cAMP was detected in tobacco leaves infiltrated with DC3000 expressing HopG1–CyaA but not with the DC3000 T3SS defective *hrcC* mutant expressing HopG1–CyaA (Fig. 1B). These data confirm that HopG1–CyaA is translocated into plant cells by the T3SS of DC3000. The expression pattern, secretion (Petnicki-Ocwieja *et al.*, 2002) and translocation of HopG1 are all hallmarks of a T3E.

To determine if HopG1 contributes to virulence we performed *in planta* growth assays with UNL124, a DC3000 *hopG1* mutant (Jamir *et al.*, 2004). We spray-inoculated *A. thaliana* Col-0 with wild-type DC3000 and the UNL124 strain and compared their growth. The UNL124 strain was not compromised in its virulence (Fig. S2). However, because DC3000 possesses greater than 30 T3Es HopG1's contribution to virulence may be masked by other T3Es that are functionally redundant.

Constitutive expression of HopG1 in plants alters development

To investigate the function of HopG1 *in planta* we made transgenic *A. thaliana* Col-0 plants that constitutively express a C-terminal haemagglutinin (HA) epitope-tagged HopG1 (HopG1–HA) using *Agrobacterium*-mediated transformation (Bechtold *et al.*, 1993). Expression of the epitope-fused HopG1 product was confirmed in *A. thaliana* Col-0 primary transformants by immunoblotting using anti-HA antibodies (Fig. S3). The *A. thaliana* Col-0 primary transformants expressing HopG1–HA were severely dwarf, highly branched and infertile (Fig. 2C and E). They also had a larger number of leaves and inflorescences (Fig. 2A) as well as increased root mass (Fig. 2E) when compared with wild-type *A. thaliana* Col-0 (Fig. 2A, B, and D). Importantly, these phenotypes were also observed in *Nicotiana tabacum* cv. Xanthi (tobacco) (Fig. 2G) and *Lycopersicon esculentum* cv. Moneymaker (tomato) (Fig. 2I) transgenic events constitutively expressing the HopG1–HA fusion protein. These data demonstrate that HopG1 expression *in planta* drastically impacts growth and development in members of the Solanaceae and Brassicaceae. These physiological changes are not seen in wild-type plants infected with DC3000. They may reflect the consequences of constitutively expressed HopG1–HA interacting with its targets in cell types that otherwise would not be presented with this T3E during the course of bacterial/host interaction. Thus, it suggests that HopG1's virulence targets may also play a role, either directly or indirectly, in plant development.

HopG1 is a suppressor of plant innate immunity

HopG1 is a suppressor of ETI, as demonstrated by a DC3000 *hopG1* mutant eliciting an enhanced HR in tobacco (Jamir *et al.*, 2004) and because HopG1 was capable of suppressing an ETI-induced HR (Guo *et al.*, 2009). To determine the extent that HopG1 could also suppress PTI responses, *A. thaliana* Col-0 plants constitutively expressing HopG1–HA were spray-inoculated with a DC3000 T3SS defective *hrcC* mutant. Due to this mutant's inability to inject T3Es, PAMP recognition by the plant results in PTI, making this strain a *de facto* PTI

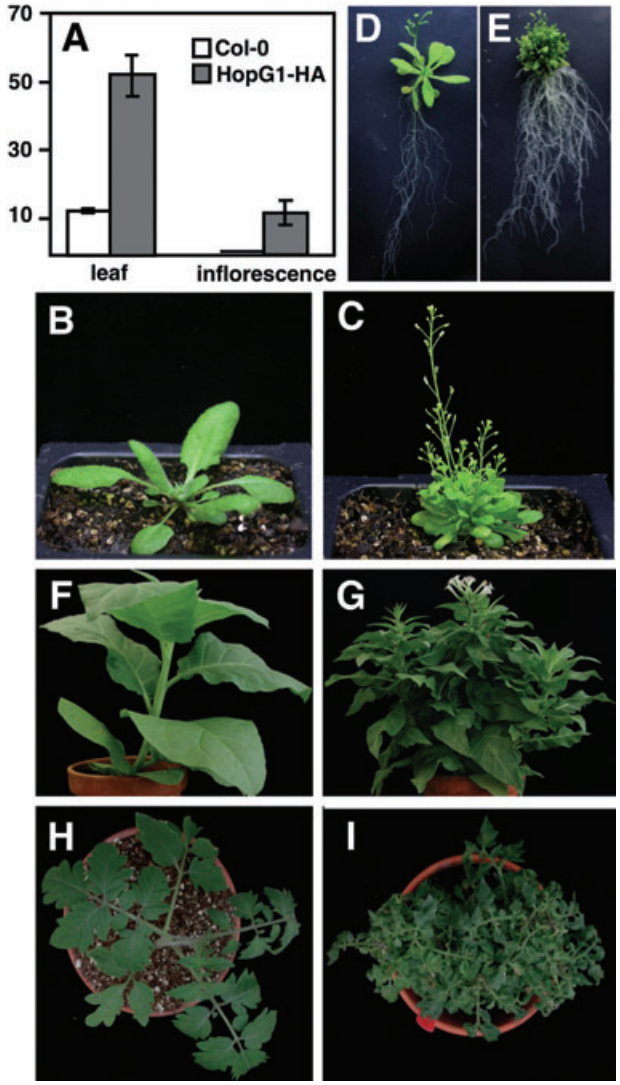

Fig. 2. The constitutive expression of DC3000 HopG1–HA *in planta* causes an altered developmental phenotype. (A) Bar graph showing the number of leaves and inflorescences on wild-type *A. thaliana* Col-0 and *A. thaliana* Col-0 expressing HopG1–HA 20 days after germination (the standard errors are indicated, $P < 0.001$). Photographs of *A. thaliana* Col-0 wild-type (B) and *A. thaliana* Col-0 expressing HopG1–HA (C) taken 20 days after germination. Five week old *A. thaliana* Col-0 wild-type (D) and *A. thaliana* Col-0 expressing HopG1–HA (E) grown on agar MS plates. *N. tabacum* cv. Xanthi (tobacco) wild-type (F) and *N. tabacum* cv. Xanthi expressing HopG1–HA (G). *L. esculentum* cv. Moneymaker (tomato) wild-type (H) and *L. esculentum* cv. Moneymaker expressing HopG1–HA (I). Constitutive expression of HopG1–HA in all of these plants led to reduced stature, increased branching, and infertility.

inducer. The HopG1–HA-expressing plants accumulated higher titres of the *hrcC* mutant than wild-type plants. A similar assay with wild-type DC3000 showed that it grew similarly in HopG1–HA-expressing plants and in wild-type plants (Fig. 3A). Taken together, these data indicate that HopG1 can suppress PTI.

To further examine the ability of HopG1 to suppress PTI the deposition of callose (β-1,3 glucan), an output of PTI, was monitored (Felix *et al.*, 1999). HopG1's impact on callose depostion was ascertained using two complementary approaches. First, the peptide Flg21 was infiltrated into wild-type *A. thaliana* Col-0 plants and plants expressing HopG1–HA. Flg21 is a conserved peptide of flagellin, which induces PTI responses due to its recognition by the PAMP receptor FLS2 (Gomez-Gomez and Boller, 2000). Callose deposits were visualized by staining with the fluorescent dye aniline blue. *A. thaliana* Col-0 plants expressing HopG1–HA had less foci stained with aniline blue than wild-type Col-0 plants, indicating that *in planta* expression of HopG1–HA suppressed callose deposition (Fig. 3B).

The second approach determined whether bacterial-delivered HopG1–HA could suppress callose deposition. The non-pathogen *P. fluorescens* (*Pf*) carrying construct pLN1965 (Wei *et al.*, 2007; Guo *et al.*, 2009), which expresses a functional T3SS from *P. syringae* pv. *syringae* 61. *Pf*(pLN1965) can inject an introduced T3E and allows the investigation of the biological activity of an individual T3E. Importantly, *Pf*(pLN1965) also induces PTI (including callose deposition) due to the presence of PAMPs found in *P. fluorescens* that are recognized by plants. An empty vector control or a construct carrying *hopG1–ha* were introduced into *Pf*(pLN1965). The resultant strains were infiltrated at a cell density of 1×10^6 cells ml^{-1} into wild-type *A. thaliana* Col-0 plants and callose deposition was measured. Indeed, callose deposition in plants infiltrated with *Pf*(pLN1965) expressing HopG1–HA was reduced compared with those infiltrated with an empty vector control (Fig. 3B). Taken together, both experimental approaches demonstrate that HopG1 can suppress PTI. Moreover, since HopG1 can also suppress ETI, it suggests that HopG1 may target components of plant immunity common to both responses.

To determine the extent that HopG1 could suppress specific PTI-induced genes we examined the expression of PR1 and WRKY22 in wild-type and HopG1–HA-expressing *A. thaliana* treated with Flg21 (Fig. 3C). This was accomplished using semi-quantitative RT-PCR. Both PR1 and WRKY22 have been shown to be induced in response to flagellin (Gomez-Gomez *et al.*, 1999; Navarro *et al.*, 2004). We found that Flg21-induced expression of both PR1 and WRKY22 was reduced in HopG1–HA-expressing plants. These data further confirm that HopG1 can suppress PTI.

HopG1 is targeted to plant mitochondria

The subcellular localization of a T3E can provide clues to its function. With this in mind we investigated the subcellular targeting of HopG1. To this end, a *hopG1* gene fusion that, when expressed, would link the C-terminus of

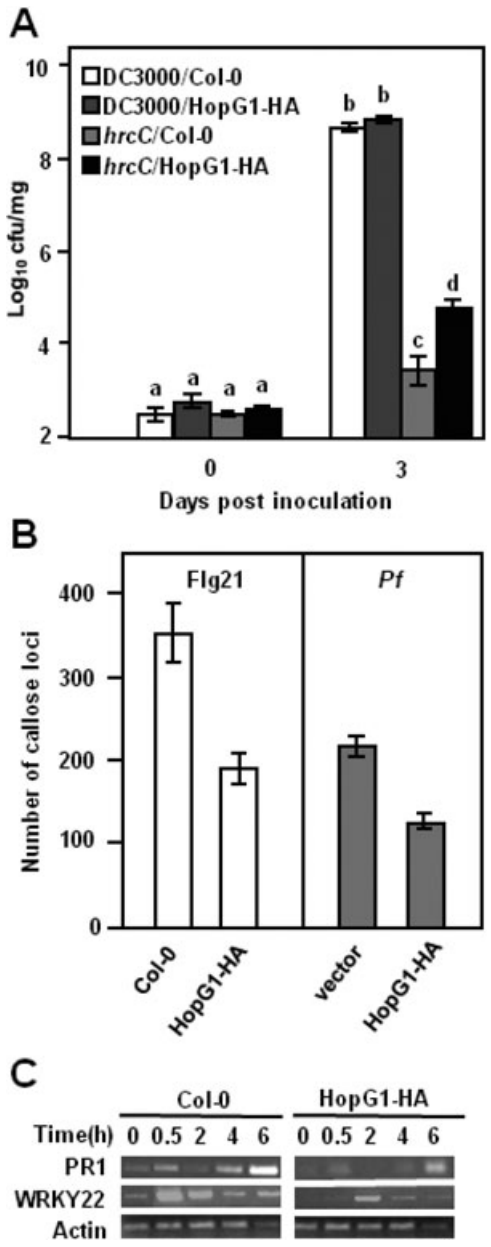

Fig. 3. HopG1–HA suppresses PTI outputs.
A. Wild-type and HopG1–HA-expressing *A. thaliana* Col-0 were spray-inoculated with 1×10^8 cells ml^{-1} of DC3000 or the DC3000 T3SS deficient *hrcC* mutant and bacteria were enumerated at 0 and 3 days after inoculation. No difference in bacterial growth was observed with DC3000 on the HopG1–HA-expressing plants, but the *hrcC* mutant showed a greater increase in growth on HopG1–HA-expressing plants compared with wild-type *A. thaliana* [a, b, c and d are statistically significantly different ($P < 0.01$), standard error is shown].
B. Wild-type and HopG1–HA-expressing *A. thaliana* Col-0 plants were infiltrated with the Flg21 peptide from flagellin or wild-type *A. thaliana* Col-0 was infiltrated with the PTI-inducing non-pathogen *P. fluorescens* (*Pf*) expressing a *P. syringae* T3SS carrying *hopG1–HA* or a vector control. The plant tissue was stained with aniline blue and callose foci were enumerated. These results showed that both *in planta* expressed HopG1–HA and T3SS-injected HopG1–HA can suppress callose deposition ($P < 0.01$). Each experiment was repeated at least twice with similar results and the standard error bars are indicated.
C. Semi-quantitative RT-PCR of pathogen induced genes from wild-type and HopG1–HA-expressing *A. thaliana* infiltrated with Flg21. PR1 and WRKY22 were downregulated in HopG1–HA-expressing plants in response to Flg21.

the protein to the green fluorescence protein (GFP) was assembled and cloned into a binary vector downstream of a constitutive 35S CaMV promoter. The resultant construct was introduced into *Agrobacterium* and the derived strain infiltrated into tobacco leaves. After 48 h the infiltrated leaves were viewed with confocal microscopy. HopG1–GFP was localized to small discrete points in the cytosol (Fig. 4A). The punctate fluorescence pattern was reminiscent of those produced by mitochondrially targeted GFP fusions (Forner and Binder, 2007).

To determine if HopG1–GFP was indeed localized to mitochondria we performed colocalization experiments with HopG1–GFP and an N-terminal mitochondrial targeting sequence from isovaleryl-CoA-dehydrogenase (IVD) fused to the red fluorescent protein eqFP611 (Forner and Binder, 2007). The nucleotide sequence corresponding to the IVD–eqFP611 was subcloned into the pZP212 binary vector. *Agrobacterium* strains carrying HopG1–GFP or IVD–eqFP611 constructs were mixed and infiltrated into tobacco leaves. After 48 h infiltrated leaves were viewed with confocal microscopy. Plant cells expressing both HopG1–GFP and IVD–eqFP611 produced punctate yellow spots in their cytoplasm, indicating that HopG1–GFP colocalized with IVD–eqFP611 and is therefore targeted to the mitochondria (Fig. 4A).

To confirm localization to the mitochondria intact organelles were isolated from wild-type and HopG1–HA-expressing tobacco leaves using Percoll density gradient fractionation. Levels of HopG1–HA in mitochondria fractions were compared with those in total protein extracts with immunoblots using anti-HA antibodies. Enrichment of HopG1–HA was observed in the mitochondrial fraction of HopG1–HA-expressing tobacco, indicating organellar localization (Fig. 4B). Control immunoblots using antibodies to alternative oxidase (AOX), a known mitochondrial protein, were performed to confirm that there was an enrichment of mitochondrial proteins in the mitochondria fractions when compared with total protein extracts. These subcellular fractionation experiments confirm that HopG1–HA is localized to the mitochondria.

To determine if the putative T3Es that share high similarity to HopG1 also localize to the mitochondria we repeated the confocal microscopy experiments with a HopG1 homologue from *X. campestris* pv. *campestris* ATCC 33913, $HopG1_{Xcc}$ (NP_638946), which is 48% identical to HopG1 (Fig. S1). A $HopG1_{Xcc}$–GFP fusion construct was introduced into *Agrobacterium* and infiltrated into tobacco leaves. The $HopG1_{Xcc}$–GFP fusion also local-

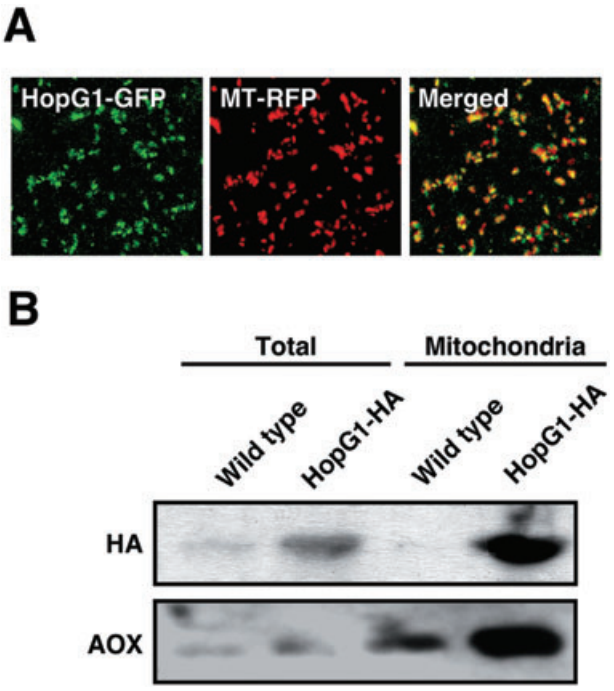

Fig. 4. HopG1 is targeted to plant mitochondria.
A. HopG1 C-terminally fused to the green fluorescence protein (HopG1–GFP) and an N-terminal mitochondrial targeting sequence from isovaleryl-CoA-dehydrogenase fused to the red fluorescent protein eqFP611 (MT–RFP) were transiently coexpressed in tobacco by *Agrobacterium*-mediated transformation and imaged using confocal microscopy. HopG1–GFP, MT–RFP and merged images are shown. The yellow fluorescence in the merged image indicates colocalization of HopG1–GFP and MT–RFP.
B. Subcellular fractionation of mitochondria from wild-type and HopG1–HA-expressing tobacco was accomplished using Percoll density gradient centrifugation and the resulting samples were analysed with immunoblots using antibodies that recognized HA or alternative oxidase (AOX). The immunoblot analysis showed that the sample from plants expressing HopG1–HA was enriched in the mitochondrial fraction compared with the total protein extract. A non-specific band of a similar size to HopG1–HA was also recognized by the anti-HA antibodies as seen in the wild-type total protein extract. Immunoblots against the classic mitochondria marker protein AOX were used to evaluate mitochondrial enrichment. Each experiment was repeated at least twice with similar results.

ized to the mitochondria as supported by the observed colocalization with IVD–eqFP611 (Fig. S4). These data indicate that the putative T3Es that share similarity with HopG1 also localize to the mitochondria and suggest that this localization is vital for their function.

The mitochondrial targeting sequence is in the N-terminus of HopG1

A conserved mitochondrial targeting sequence was not identified within the 492-amino-acid-long HopG1 protein using bioinformatics tools. To define a region within HopG1 that is required for mitochondrial targeting we made truncated versions of HopG1 fused C-terminally to GFP. These proteins were transiently expressed in tobacco and subsequently imaged using confocal microscopy. The N-terminal regions spanning amino acids 1–263 or 1–380 of HopG1 fused to GFP displayed mitochondrial localization indicating that the N-terminal 263 amino acids of HopG1 are sufficient for mitochondrial targeting (Fig. 5A and B). HopG1 regions encompassing amino acids 1–160, 14–492, 100–200, 160–492 or 263–492 fused to GFP localized to the cytoplasm and nucleus in a manner similar to that of the GFP control (Fig. 5A and B). The expression and size of all fusion proteins were confirmed with protein blots using anti-GFP antibodies (data not shown). Note that the chloroplasts in some images appear yellow due to the low level of accumulation of full-length HopG1–GFP that necessitated the use of detection conditions for GFP that also detected chlorophyll autofluorescence. In addition, a site-directed mutant in the putative cyclophilin binding site (Fig. S1) of HopG1–GFP that has an alanine in position 350 of the peptide instead of a glycine ($HopG1_{G350A}$–GFP) retained its ability to target the mitochondria (Fig. 5A and B). This suggests that cyclophilin binding is not required for the production of HopG1 *in planta* or its mitochondrial localization.

Combined these data indicate that the mitochondrial targeting signal of HopG1 is within its N-terminal 263 amino acids. Moreover, the failure of the HopG1–GFP fusion lacking the N-terminal 13 amino acids to be targeted to the mitochondria clearly shows that the N-terminus of HopG1 is important for mitochondrial localization (Fig. 5A and B). Consistent with this, an N-terminal GFP fusion to full-length HopG1 also localized to the cytoplasm and nucleus, suggesting that mitochondrial localization requires a free HopG1 N-terminus (data not shown). These data suggest that regions in the first 263 amino acids as well as a free HopG1 N-terminus are necessary for mitochondrial localization.

HopG1–GFP truncations do not alter plant development

To test the hypothesis that mitochondrial localization is important for the function of HopG1 we determined which regions of HopG1 were necessary to cause the altered plant development observed in transgenic plants constitutively expressing HopG1–HA (Fig. 2). To accomplish this, constructs corresponding to full-length HopG1–GFP, and the respective HopG1–GFP fusions described above, along with the $HopG1_{G350A}$–GFP amino acid substitution derivative were stably transformed into *A. thaliana* Col-0 plants via *Agrobacterium*-mediated transformation. The resulting seeds for each transgenic plant were germinated on selective medium and acclimated to soil. Expression of the HopG1–GFP derivatives was confirmed by immunoblot analysis with anti-GFP antibodies (data not shown). The derived transgenic events were assessed for the

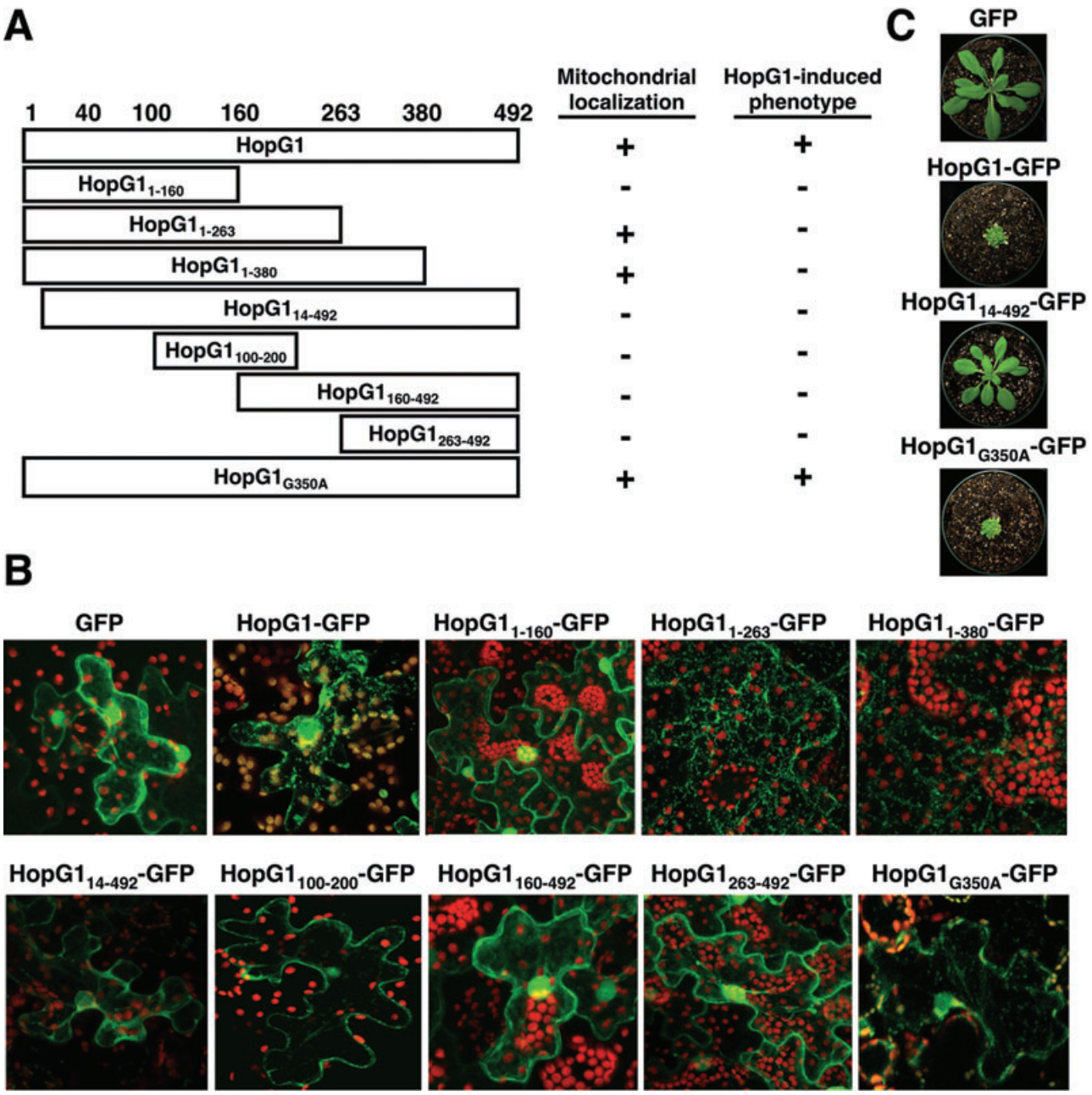

Fig. 5. The mitochondrial targeting sequence of HopG1 is in its N-terminal 263 amino acids.
A. A schematic representation of the HopG1–GFP truncations and the HopG1–GFP cyclophilin binding site mutant derivative ($HopG1_{G350A}$–GFP), their localization to plant mitochondria and ability to induce the *A. thaliana* developmental phenotype induced by full-length HopG1–HA.
B. Confocal micrographs of tobacco cells transiently expressing HopG1–GFP truncations and $HopG1_{G350A}$–GFP. Only the full-length HopG1–GFP, $HopG1_{1-263}$–GFP, $HopG1_{1-380}$–GFP and $HopG1_{G350A}$–GFP were targeted to the mitochondria. Each construct was tested at least twice with similar results.
C. HopG1–GFP truncations and $HopG1_{G350A}$–GFP were stably transformed into *A. thaliana* Col-0 to test whether they produced the HopG1-induced plant phenotype. Only full-length HopG1–GFP and $HopG1_{G350A}$–GFP induced the plant developmental phenotype as shown in these representative 4-week-old plants.

HopG1-induced developmental phenotype. Transgenic plants constitutively expressing full-length HopG1–GFP produced the same developmental phenotype as those expressing HopG1–HA (Fig. 5A and C). All plants expressing HopG1–GFP truncations resembled wild-type *A. thaliana* Col-0, indicating that HopG1 derivatives were no longer capable of inducing this phenotype (Fig. 5A and C). Importantly, the HopG1–GFP truncations that did not

localize to the mitochondria did not produce the plant phenotype. On the other hand, HopG1$_{G350A}$–GFP went to the mitochondria and produced the HopG1-induced developmental phenotype. Particularly noteworthy is that the developmental phenotype is not induced by HopG1$_{14-492}$–GFP that lacks only the N-terminal 13 amino acids of HopG1 and does not localize to the mitochondria (Fig. 5). We also determined if the mitochondrial targeting of HopG1 was necessary for the ability of HopG1 to suppress PTI. To accomplish this, the deposition of Flg21 induced callose in transgenic *A. thaliana* expressing HopG1 truncations fused to GFP was examined. When compared with plants expressing GFP alone, plants expressing HopG1–GFP had 47 ± 5% less callose and plants expressing HopG1$_{G350A}$–GFP had 68 ± 4% less callose. In contrast, plants expressing HopG1$_{1-380}$–GFP or HopG1$_{160-492}$–GFP displayed similar callose deposition to plants expressing GFP alone, 5 ± 7% less and 20 ± 10% more, respectively. These results suggest that both mitochondrial targeting and an activity in the C-terminus of HopG1 are required for HopG1's activity.

HopG1 alters respiration and ROS accumulation

The localization of HopG1 to plant mitochondria implies that mitochondria are involved in HopG1's ability to suppress innate immunity. HopG1 may suppress innate immunity by altering mitochondrial functions, such as the rate of respiration. Therefore, we determined if HopG1–HA altered basal respiration by measuring the rate of oxygen consumption of leaf disks of wild-type and HopG1–HA-expressing tobacco in the dark. The rate of oxygen consumption of tobacco expressing HopG1–HA was approximately half that of wild-type tobacco (Fig. 6A), suggesting that HopG1 impairs mitochondrial respiration and thus may cause mitochondrial dysfunction.

Restriction of mitochondrial respiration can lead to an increased production of reactive oxygen species (ROS) (Maxwell *et al*., 1999). To determine if this is the case in HopG1–HA-expressing tobacco we compared its steady-state ROS levels to those of wild-type tobacco. Relative ROS levels were determined using the ROS-sensitive fluorescent probe 2′7′-dichlorodihydrofluorescin (H2DCFHDA). Tobacco plants expressing HopG1–HA produced approximately fourfold higher basal levels of ROS than wild-type tobacco plants (Fig. 6B). These data show that the expression of HopG1–HA does result in increased ROS production in tobacco. These enhanced ROS levels may be due to altered mitochondrial functions in HopG1–HA-expressing plants.

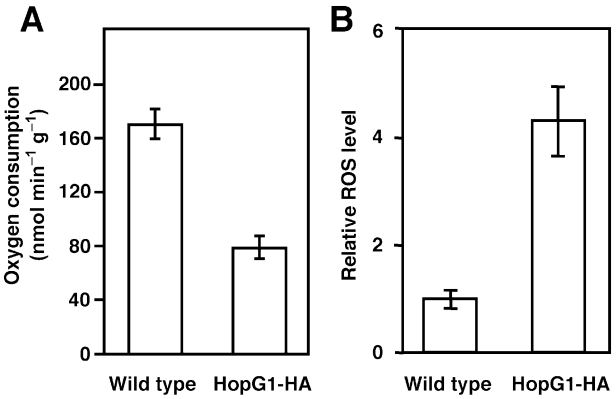

Fig. 6. Plants expressing HopG1–HA exhibit a reduced rate of respiration and increased reactive oxygen species production.
A. Oxygen consumption rates in untreated wild-type tobacco and HopG1–HA-expressing tobacco leaf disks were measured in the dark using an oxygen electrode. The rate of oxygen consumption was lower in HopG1–HA-expressing plants ($P < 0.0005$).
B. Relative basal reactive oxygen species (ROS) levels were determined in wild-type and HopG1–HA-expressing tobacco leaf extracts by measurement of the relative fluorescence of the ROS-sensitive probe H2DCFDA and normalizing to total protein content. ROS levels were enhanced in HopG1–HA-expressing plants ($P < 0.005$). Each experiment was repeated at least twice with similar results and standard errors are indicated.

Discussion

In this study, we show that the DC3000 *hopG1* gene is expressed under T3SS-inducing conditions and a HopG1–CyaA fusion is injected into plant cells (Fig. 1). This confirms an earlier report using a different translocation assay, which HopG1 is translocated (Petnicki-Ocwieja *et al*., 2002). A DC3000 mutant lacking HopG1 was not detectably reduced in virulence compared with wild-type DC3000 (Fig. S2). We have previously reported that HopG1 can suppress ETI (Jamir *et al*., 2004; Guo *et al*., 2009). We extended this finding here by showing that that HopG1 can also suppress PTI (Fig. 3). Thus, HopG1 is a suppressor of both the PTI and ETI branches of plant innate immunity. Given this significant activity it seems likely that the lack of a virulence phenotype for the DC3000 *hopG1* mutant is due to the presence of other functionally redundant T3Es. Several *P. syringae* T3Es have now been characterized for their ability to suppress PTI or ETI. An emerging theme appears to be that many T3Es can suppress both immunity branches. Perhaps this is reasonable to expect since many T3Es have multiple activities and that ETI and PTI share many of their signalling components and response outputs (Tao *et al*., 2003; Navarro *et al*., 2004).

The HopG1-induced plant developmental phenotype observed in transgenic *A. thaliana*, tomato, and tobacco (Fig. 2) is intriguing and warrants further discussion. We view phenotypes caused by the transgenic expression of T3Es as potential clues to their activities because they may be caused by the enzymatic activity of the T3E or be due to the effect the T3E has on a plant target or targets. The fact that we were unable to separate the plant phe-

notype induced by HopG1 from the localization of HopG1 to mitochondria suggests that the phenotype is associated with the site of action of HopG1 and not simply due to non-specific activity. Moreover, alterations in plant development can be associated with impaired mitochondrial function. This is particularly true for defects in fertility such as cytoplasmic male sterility, but occasionally alterations in plant growth rates and architecture are also observed (Shedge *et al*., 2007). However, we cannot, at this point, be certain that the HopG1-induced developmental phenotype is connected to HopG1's virulence role. One possibility that we are currently exploring is whether HopG1 modulates plant hormone levels. Many different hormones control plant growth and/or biotic stress responses. These hormones include ABA, ethylene, jasmonic acid, brassinosteriods, gibberellins, auxins and SA. They work in complex and finely balanced networks, which several T3Es and toxins have been shown to disrupt to the advantage of the pathogen (see Grant and Jones, 2009; Pieterse *et al*., 2009; Santner *et al*., 2009 for recent reviews). It is quite possible, perhaps even likely, that the modified developmental phenotype of HopG1-expressing plants is due to an effect on one or more of these networks.

To our knowledge HopG1 is the first plant pathogen T3E shown to localize to plant mitochondria. HopG1 lacks a predictable mitochondrial targeting sequence; however, our studies here showed that amino acids 1–263 of HopG1 were sufficient for localization to the mitochondria (Fig. 5). Neither amino acids 1–160, 14–492, 100–200 nor 160–492 of HopG1 were sufficient for mitochondrial localization, suggesting that a fairly large portion of the protein is required for mitochondrial targeting. This targeting could occur directly or be due to the interaction of HopG1 with a host protein that is targeted to the mitochondria. Mitochondrial targeting without a predictable targeting sequence is not uncommon as several bacterial pathogenicity factors imported into animal mitochondria do not have these targeting sequences (Kozjak-Pavlovic *et al*., 2008).

Our bioinformatic analyses identified a putative cyclophilin binding site in HopG1. These sites have been found in the *P. syringae* T3E AvrRpt2, where they are required for this effector to be processed *in planta* and for its cysteine protease activity (Coaker *et al*., 2005; 2006). The putative cyclophilin binding site present in HopG1 was not required for the HopG1-induced plant phenotype or mitochondrial localization. However, it is possible that our assays may not have detected a reduction in properly folded HopG1 as long as there was enough to detect its localization to mitochondria and to cause the associated phenotype.

To determine if HopG1 can alter mitochondrial function we measured the effect of HopG1 on respiration a common marker of altered mitochondria function. We demonstrated that the expression of HopG1–HA in tobacco leaves leads to a decrease in the rate of oxygen consumption coupled with enhanced basal levels of ROS. These data are consistent with the hypothesis that HopG1 alters mitochondrial function although they cannot rule out that the alteration of respiration is a secondary effect in the HopG1–HA-expressing plants. Additional experiments are required to determine the exact site and immediate consequences of HopG1 action.

Mitochondria are also involved in plant innate immunity signalling pathways (Maxwell *et al*., 2002). Thus, HopG1's ability to suppress plant innate immunity may be due to its ability to alter mitochondrial function. One possible outcome of HopG1's interaction with mitochondria is PCD suppression. PCD is a common response to pathogen infection for both resistant and susceptible hosts (Greenberg and Yao, 2004) and mitochondria play a major role in regulating it (Lam *et al*., 2001). There is a precedent for T3Es acting to alter PCD responses at the mitochondrial level. For example, bacterial pathogens of animals have been shown to prevent apoptosis by activating cell survival signals, degrading pro-apoptotic proteins, and protecting mitochondria (see Faherty and Maurelli, 2008 for a recent review). We have previously shown that HopG1 can suppress the HR and prevent Bax-induced cell death in yeast and tobacco (Jamir *et al*., 2004). Bax is thought to initiate PCD by interacting with mitochondria to cause the release of pro-apoptotic factors (Jurgensmeier *et al*., 1998). Our current data indicate that HopG1 localizes to the mitochondria and suppresses plant innate immunity. Thus, it is possible that HopG1 does so by directly protecting mitochondria from the action or release of pro-apoptotic factors.

Other plant pathogens have T3Es that have high identity to HopG1, suggesting that these are broadly important T3Es. At least one of these is also localized to the mitochondria (Fig. S4). Thus, our findings reveal a novel site of action for a plant pathogen T3E and suggest that plant pathogens target mitochondria to disable plant immunity.

Experimental procedures

RT-PCR analysis

DC3000 strains were grown in King's B (KB) broth (King *et al*., 1954) and T3SS-inducing minimal media (Yuan and He, 1996) with the appropriate antibiotics at 22°C for 3 h, and the cells were harvested at log phase. Transgenic *A. thaliana* plants were infiltrated with 10 μM Flg21 and tissue was harvested 16 h later. Total RNA was purified using RNeasy mini Kit (QIAGEN, http://www.qiagen.com). Extensive DNase treatment of the RNA was performed with DNA-free (Ambion, http://www.ambion.com). The reverse transcription of RNA was carried out using RETROscript

(Ambion, http://www.ambion.com) using oligo (dT) primers with heat denaturation of the RNA. *hopG1* was amplified using primers 5′-CACCATGCAAATAAAGAACAGTCATCTC-3′ (P2887) and 5′-GCCGTTGTAAAACTGCTTAGAGG-3′ (P2890). *hrpL* was amplified using primers 5′-AGTGAATTCATGTTTCAGAAGAT TGTG-3′ (P1626) and 5′-AGTCTCGAGTCAGGCGAACGGG TCGAT-3′ (P1627). PCR conditions were 30 cycles of 94°C for 30 s, 50°C for 30 s and 72°C for 1.5 min followed by an extension of 72°C for 10 min. *Actin* was amplified using primers 5′-CTAAGCTCTCAAGATCAAAAGGC-3′ (P2228) and 5′-TTA ACATTGCAAAGAGTTTCAAGG-3′ (P2229). *PR1* was amplified using primers 5′-TGAATTTTACTGGCTATTCTCG-3′ (P1268) and 5′-TCTCCAAACAACTTGAGTGT-3′ (P1269). WRKY22 was amplified using primers 5′-CACCAACAATGGCCGACGATTG GGATCTC-3′ (P1475) and 5′-TATTCCTCCGGTGGTAGTG-3′ (P1476). PCR conditions were 30 cycles of 94°C for 10 s, 52°C for 30 s and 72°C for 30 s followed by an extension of 72°C for 5 min.

Adenylate cyclase (CyaA) translocation assay

A construct encoding a HopG1 C-terminal CyaA fusion was made by the recombination of pENTR/D-TOPO::*hopG1* with the Gateway vector pLN2193 (Fu *et al.*, 2006). It was then transformed into DC3000 and *hrcC* strains by electroporation. The CyaA assays were performed following a previously described protocol (Schechter *et al.*, 2004). Briefly, freshly grown bacteria from plates were suspended in 5 mM morpholinoethanesulfonic acid (MES), pH 5.6, at an OD_{600} of 0.5. Then the bacterial suspensions were infiltrated into *N. benthamiana* leaves. Leaf disks of 0.9 cm in diameter were harvested 7 h after infiltration and ground in liquid nitrogen and resuspended in 0.1 M HCl. A direct cyclic AMP (cAMP) correlate enzyme immunoassay kit (Assay Designs, http://www.assaydesigns.com) was used to measure cAMP concentrations in each sample following the manufacturer's instructions.

Transgenic plant production

Transgenic plants constitutively expressing HopG1 were made by *Agrobacterium*-mediated plant transformation with pPZP212:*hopG1–HA* (pLN530) (Jamir *et al.*, 2004) or the pK7FWG2:*hopG1* constructs. *A. thaliana* Col-0 plants were transformed by floral dip (Bechtold *et al.*, 1993). Tobacco and tomato transformations were carried out as described (Horsch *et al.*, 1985; McCormick *et al.*, 1986). Experiments were performed at least twice with similar results using at least four primary transformants for each construct. Transgene accumulation was determined by Western blotting, RT-PCR and/or confocal microscopy.

A. thaliana *pathogenicity assays*

DC3000, the DC3000 *hopG1* mutant (UNL124) (Jamir et al., 2004), and the DC3000 *hrcC* mutant (Yuan and He, 1996) were grown overnight at 30°C on KB agar plates with the appropriate antibiotics and bacterial suspensions were made to an OD_{600} of 0.2 in 10 mM $MgCl_2$ containing 0.02% (v/v) silwet (Lehle Seeds, http://www.arabidopsis.com). *A. thaliana* Col-0 plants grown for 4 weeks at 25°C on 10 h days were covered with a humidity dome overnight and then sprayed with a fine mist of the bacterial suspension. One-square-centimetre leaf disks were sampled from the infected tissue and ground in 10 mM $MgCl_2$. The plating of serial dilutions of the samples on KB agar with the appropriate antibiotics allowed the number of colony forming units (cfu) of DC3000 in the leaf tissue to be determined. ANOVA was performed for all appropriate experiments.

Callose deposition assay

For assaying Flg21-induced callose deposition, wild-type *A. thaliana* Col-0, HopG1–HA, HopG1–GFP and HopG1–GFP truncation transgenic plants were infiltrated with 10 μM Flg21. For assaying callose deposition induced by *P. fluorescens (Pf)*, wild-type *A. thaliana* Col-0 was infiltrated with 10^8 cells ml^{-1} of *Pf*(pLN1965) carrying pML123 or pML123:*hopG1–HA*. Sixteen hours after infiltration leaf samples were cleared with alcoholic lactophenol, rinsed with 50% ethanol (v/v) followed by water as described (Adam and Somerville, 1996). The completely cleared leaves were stained with 0.01% aniline blue (w/v) in a solution of 150 mM K_2HPO_4, pH 9.5, for 30 min. The callose deposits were visualized with a Zeiss Axionplan 2 imaging Microscope. QUANTITY ONE software (Bio-Rad, http://www.bio-rad.com) was used to enumerate callose deposits.

HopG1 immunofluorescence assays

HopG1 truncated constructs were made by amplifying *hopG1* from DC3000 total DNA by PCR with Pfu polymerase using 30 cycles of 94°C for 1 min, 52°C for 1 min and 72°C for 1.5 min followed by an extension of 72°C for 10 min. The following primers were used for the gene truncations and the corresponding amino acid location of the primer and its primer number are in the parenthesis: 5′-CACCATGCAAATAAAGAACAGTCATCTC-3′ ($HopG1_1$, P2887), 5′-CACCCTCGAGATGGTGCAGAATACTTTT AATG-3′ ($HopG1_{14}$, P3498), 5′-CACCATGGGTGGTTTTACCAG CGATGCCAGG-3′ ($HopG1_{100}$, 3014), 5′-CACCATGTCCGACC TAGTTGACACGGAGC-3′ ($HopG1_{160}$, P3015), 5′-CACCATGGA AACTCTTGATAACTTACTTCG-3′ ($HopG1_{263}$, P2889), 5′-GGAG AGGTAAATCTTAGTTGC-3′ ($HopG1_{160}$, P2964), 5′-GTCTTTT GGTGTTTTTTCCGGGT-3′ ($HopG1_{200}$, P2965), 5′-CATTGATTT ATGTTTCAAATCTTCTATTTT-3′ ($HopG1_{263}$, P2888), 5′-CATT GATTTATGTTTCAAATCTTCTATTTT-3′ ($HopG1_{380}$, P2886), and 5′-GCCGTTGTAAAACTGCTTAGAGG-3′ ($HopG1_{492}$, P2890). PCR products were placed into pENTR/D-TOPO (Invitrogen, http://www.invitrogen.com) and then recombined into pK7FWG2 (Karimi *et al.*, 2002) to create constructs that express C-terminal GFP fusion proteins. These were then transiently expressed in tobacco leaves by *Agrobacterium*-mediated transformation (Jamir *et al.*, 2004). Localization of GFP fusions was visualized with sequential laser scanning confocal microscopy, using an Olympus FV500 with sequential imaging at 488 nm excitation and 505–525 nm emission (green/GFP) and 633 nm excitation and 660 nm emission (red/chlorophyll). The $HopG1_{G350A}$ cyclophilin binding site mutant was made by using the QuickChange™ site-directed mutagenesis kit (Stratagene, http://www.stratagene.com) to change the codon GGG to GCC on pENTR/D-TOPO::$hopG1_{1\text{-}492}$ with the primers 5′-GGAATACCAGCATT GCAGCCCCAGTGCTCTACCACGC-3′ (P3008) and 5′-GCGT GGTAGAGCACTGGGGCTGCAATGCTGGTATTCC-3′ (P3009).

Colocalization with mitochondria was performed with pIVD–eqFP611 (Forner and Binder, 2007) that was cloned in a Gateway version of pPZP212 using the primers 5′-CACCATGCAGAG GTTTTTCTCCGC-3′ (P3415) and 5′-TCAAAGACGTCCCAGT TTGG-3′ (P3040) for *Agrobacterium*-mediated transformation. Laser scanning confocal microscopy with 543 nm excitation and 560–600 nm emission wavelengths was used to visualize the IVD–eqFP611 fusion protein.

Subcellular fractionation

Fifty grams of tobacco leaf tissue was shredded and gently disrupted with a mortar and pestle in 120 ml of extraction medium (EM) 20 mM Hepes-Tris, pH 7.6, 0.4 M sucrose, 5 mM EDTA, 0.6% PVP (w/v, 0.6 mM cysteine). The extract was filtered through eight layers of cheesecloth and centrifuged 5 min at 3500 g. The supernatant was centrifuged at 28 000 *g* for 10 min to pellet organelles. The pellet was resuspended in 120 ml EM without PVP and centrifuged at 28 000 *g* for 10 min and the pellet resuspended in 2 ml of suspension buffer (SB) 10 mM MOPS-KOH, pH 7.2, 0.2 M sucrose and loaded on a Percoll gradient of 10%, 32% and 50% percoll in SB. The gradient was centrifuged at 40 000 *g* and the mitochondria collected as a band between the 32% and 50% percoll stages. The mitochondrial fraction was washed three times in two volumes of SB by centrifugation at 16 000 *g* for 40 min. Protein blots were performed with anti-HA antibodies (Roche, http://www.roche.com) and anti-AOX antibodies (Elthon *et al*., 1989).

Oxygen consumption

One-square-centimetre leaf disks were cut from wild-type tobacco and tobacco constitutively expressing HopG1–HA. Oxygen consumption was measured polarographically using a Rank Brothers oxygen electrode (Rank Brothers, http://www.rankbrothers.co.uk) at 25°C in 1 ml of air-saturated water in the dark. Each experiment was done with three replicates.

ROS measurement

Leaf tissue from wild-type tobacco and tobacco constitutively expressing HopG1–HA was ground in liquid nitrogen and resuspended in ice-cold 10 mM Tris-HCl, pH 7.3. Samples were centrifuged twice to remove cell debris and 0.1 ml of the supernatant was placed in duplicate on a Microfluor®1 white wellplate (Thermo Scientific, http://www.thermofisher.com). 2′-7′-dichlorodihydrofluorescein diacetate (H2DCFDA, Invitrogen, http://www.Invitrogen.com) to a final concentration of 10 μM was added to the wells and mixed. Fluorescence was measured with an excitation wavelength of 485 nm and an emission wavelength of 535 nm on a CaryEcilpse fluorometer. Protein content was determined by the Bradford assay and relative basal ROS levels calculated with wild-type tobacco were set to 1.

Acknowledgements

We thank members of the Alfano laboratory for many fruitful discussions regarding HopG1 and in particular Matt Dale for his assistance with experiments. We thank Thomas Elthon for the anti-AOX antibodies, Stefan Binder for IVD–eqFP611 and Fang Tian for the CyaA assays. We also thank Thomas Elthon and Sally Mackenzie for advice about our experiments with plant mitochondria. This research was supported by grants from the National Science Foundation (Award No. MCB-0544447), United States Department of Agriculture 2007-35319-18336, and the National Institutes of Health (Award No. 1R01AI069146-01A2) and funds from the Center for Plant Science Innovation at the University of Nebraska.

References

Abramovitch, R.B., Kim, Y.J., Chen, S., Dickman, M.B., and Martin, G.B. (2003) *Pseudomonas* type III effector AvrPtoB induces plant disease susceptibility by inhibition of host programmed cell death. *EMBO J* **22:** 60–69.

Abramovitch, R.B., Anderson, J.C., and Martin, G.B. (2006) Bacterial elicitation and evasion of plant innate immunity. *Nat Rev Mol Cell Biol* **7:** 601–611.

Adam, L., and Somerville, S.C. (1996) Genetic characterization of five powdery mildew disease resistance loci in *Arabidopsis thaliana*. *Plant J* **9:** 341–356.

Alfano, J.R., and Collmer, A. (2004) Type III secretion system effector proteins: double agents in bacterial disease and plant defense. *Annu Rev Phytopathol* **42:** 385–414.

Alfano, J.R., Charkowski, A.O., Deng, W., Badel, J.L., Petnicki-Ocwieja, T., van Dijk, K., and Collmer, A. (2000) The *Pseudomonas syringae* Hrp pathogenicity island has a tripartite mosaic structure composed of a cluster of type III secretion genes bounded by exchangeable effector and conserved effector loci that contribute to parasitic fitness and pathogenicity in plants. *Proc Natl Acad Sci USA* **97:** 4856–4861.

Ausubel, F.M. (2005) Are innate immune signaling pathways in plants and animals conserved? *Nat Immunol* **6:** 973–979.

Bechtold, N., Ellis, J., and Pelletier, G. (1993) In planta *Agrobacterium* mediated gene transfer by infiltration of adult *Arabidopsis thaliana* plants. *C R Acad Sci Paris* **316:** 1194–1199.

Block, A., Li, G., Fu, Z.Q., and Alfano, J.R. (2008) Phytopathogen type III effector weaponry and their plant targets. *Curr Opin Plant Biol* **11:** 396–403.

Chisholm, S.T., Coaker, G., Day, B., and Staskawicz, B.J. (2006) Host–microbe interactions: shaping the evolution of the plant immune response. *Cell* **124:** 803–814.

Coaker, G., Falick, A., and Staskawicz, B. (2005) Activation of a phytopathogenic bacterial effector protein by a eukaryotic cyclophilin. *Science* **308:** 548–550.

Coaker, G., Zhu, G., Ding, Z., Van Doren, S.R., and Staskawicz, B. (2006) Eukaryotic cyclophilin as a molecular switch for effector activation. *Mol Microbiol* **61:** 1485–1496.

Cunnac, S., Lindeberg, M., and Collmer, A. (2009) *Pseudomonas syringae* type III secretion system effectors: repertoires in search of functions. *Curr Opin Microbiol* **12:** 53–60.

Elthon, T.E., Nickels, R.L., and McIntosh, L. (1989) Monoclonal antibodies to the alternative oxidase of higher plant mitochondria. *Plant Physiol* **89:** 1311–1317.

Espinosa, A., and Alfano, J.R. (2004) Disabling surveillance:

bacterial type III secretion system effectors that suppress innate immunity. *Cell Microbiol* **6:** 1027–1040.
Faherty, C.S., and Maurelli, A.T. (2008) Staying alive: bacterial inhibition of apoptosis during infection. *Trends Microbiol* **16:** 173–180.
Felix, G., Duran, J.D., Volko, S., and Boller, T. (1999) Plants have a sensitive perception system for the most conserved domain of bacterial flagellin. *Plant J* **18:** 265–276.
Forner, J., and Binder, S. (2007) The red fluorescent protein eqFP611: application in subcellular localization studies in higher plants. *BMC Plant Biol* **7:** 28.
Fu, Z.Q., Guo, M., and Alfano, J.R. (2006) *Pseudomonas syringae* HrpJ is a type III secreted protein that is required for plant pathogenesis, injection of effectors, and secretion of the HrpZ1 harpin. *J Bacteriol* **188:** 6060–6069.
Gomez-Gomez, L., and Boller, T. (2000) FLS2: an LRR receptor-like kinase involved in the perception of the bacterial elicitor flagellin in *Arabidopsis*. *Mol Cell* **5:** 1003–1011.
Gomez-Gomez, L., Felix, G., and Boller, T. (1999) A single locus determines sensitivity to bacterial flagellin in *Arabidopsis thaliana*. *Plant J* **18:** 277–284.
Grant, M.R., and Jones, J.D. (2009) Hormone (dis) harmony moulds plant health and disease. *Science* **324:** 750–752.
Greenberg, J.T., and Yao, N. (2004) The role and regulation of programmed cell death in plant–pathogen interactions. *Cell Microbiol* **6:** 201–211.
Guo, M., Tian, F., Wamboldt, Y., and Alfano, J.R. (2009) The majority of the type III effectory inventory of *Pseudomonas syringae* pv. *tomato* DC3000 can suppress plant immunity. *Mol Plant Microbe Interact* **22:** 1069–1080.
Horsch, R.B., Fry, J.E., Hoffmann, N.L., Eichholtz, D., Rogers, S.G., and Fraley, R.T. (1985) A simple and general method for transferring genes into plants. *Science* **227:** 1229–1231.
Jamir, Y., Guo, M., Oh, H.-S., Petnicki-Ocwieja, T., Chen, S., Tang, X., *et al.* (2004) Identification of *Pseudomonas syringae* type III effectors that suppress programmed cell death in plants and yeast. *Plant J* **37:** 554–565.
Jelenska, J., Yao, N., Vinatzer, B.A., Wright, C.M., Brodsky, J.L., and Greenberg, J.T. (2007) A J domain virulence effector of *Pseudomonas syringae* remodels host chloroplasts and suppresses defenses. *Curr Biol* **17:** 499–508.
Jones, J.D., and Dangl, J.L. (2006) The plant immune system. *Nature* **444:** 323–329.
Jurgensmeier, J.M., Xie, Z., Deveraux, Q., Ellerby, L., Bredesen, D., and Reed, J.C. (1998) Bax directly induces release of cytochrome *c* from isolated mitochondria. *Proc Natl Acad Sci USA* **95:** 4997–5002.
Karimi, M., Inze, D., and Depicker, A. (2002) GATEWAY vectors for *Agrobacterium*-mediated plant transformation. *Trends Plant Sci* **7:** 193–195.
King, E.O., Ward, M.K., and Raney, D.E. (1954) Two simple media for the demonstration of pyocyanin and fluorescein. *J Lab Med* **22:** 301–307.
Kozjak-Pavlovic, V., Ross, K., and Rudel, T. (2008) Import of bacterial pathogenicity factors into mitochondria. *Curr Opin Microbiol* **11:** 9–14.
Lam, E., Kato, N., and Lawton, M. (2001) Programmed cell death, mitochondria and the plant hypersensitive response. *Nature* **411:** 848–853.
Lewis, J.D., Abada, W., Ma, W., Guttman, D.S., and Desveaux, D. (2008) The HopZ family of *Pseudomonas syringae* type III effectors require myristoylation for virulence and avirulence functions in *Arabidopsis thaliana*. *J Bacteriol* **190:** 2880–2891.
Lindeberg, M., Cartinhour, S., Myers, C.R., Schechter, L.M., Schneider, D.J., and Collmer, A. (2006) Closing the circle on the discovery of genes encoding Hrp regulon members and type III secretion system effectors in the genomes of three model *Pseudomonas syringae* strains. *Mol Plant Microbe Interact* **19:** 1151–1158.
McCormick, S., Niedermeyer, J., Fry, J., Barnason, A., Horsch, R., and Fraley, R. (1986) Leaf disc transformation of cultivated tomato (*L. esculentum*) using *Agrobacterium tumefaciens*. *Plant Cell Reports* **5:** 81–84.
Maxwell, D.P., Wang, Y., and McIntosh, L. (1999) The alternative oxidase lowers mitochondrial reactive oxygen production in plant cells. *Proc Natl Acad Sci USA* **96:** 8271–8276.
Maxwell, D.P., Nickels, R., and McIntosh, L. (2002) Evidence of mitochondrial involvement in the transduction of signals required for the induction of genes associated with pathogen attack and senescence. *Plant J* **29:** 269–279.
Navarro, L., Zipfel, C., Rowland, O., Keller, I., Robatzek, S., Boller, T., and Jones, J.D. (2004) The transcriptional innate immune response to flg22. Interplay and overlap with Avr gene-dependent defense responses and bacterial pathogenesis. *Plant Physiol* **135:** 1–16.
Nimchuk, Z., Marois, E., Kjemtrup, S., Leister, R.T., Katagiri, F., and Dangl, J.L. (2000) Eukaryotic fatty acylation drives plasma membrane targeting and enhances function of several type III effector proteins from *Pseudomonas syringae*. *Cell* **101:** 353–363.
Nurnberger, T., Brunner, F., Kemmerling, B., and Piater, L. (2004) Innate immunity in plants and animals: striking similarities and obvious differences. *Immunol Rev* **198:** 249–266.
Oh, H.S., and Collmer, A. (2005) Basal resistance against bacteria in *Nicotiana benthamiana* leaves is accompanied by reduced vascular staining and suppressed by multiple *Pseudomonas syringae* type III secretion system effector proteins. *Plant J* **44:** 348–359.
Petnicki-Ocwieja, T., Schneider, D.J., Tam, V.C., Chancey, S.T., Shan, L., Jamir, Y., *et al.* (2002) Genomewide identification of proteins secreted by the Hrp type III protein secretion system of *Pseudomonas syringae* pv. *tomato* DC3000. *Proc Natl Acad Sci USA* **99:** 7652–7657.
Pieterse, C.M., Leon-Reyes, A., Van der Ent, S., and Van Wees, S.C. (2009) Networking by small-molecule hormones in plant immunity. *Nat Chem Biol* **5:** 308–316.
Robert-Seilaniantz, A., Shan, L., Zhou, J.M., and Tang, X. (2006) The *Pseudomonas syringae* pv. *tomato* DC3000 type III effector HopF2 has a putative myristoylation site required for its avirulence and virulence functions. *Mol Plant Microbe Interact* **19:** 130–138.
Santner, A., Calderon-Villalobos, L.I., and Estelle, M. (2009) Plant hormones are versatile chemical regulators of plant growth. *Nat Chem Biol* **5:** 301–307.

Schechter, L.M., Roberts, K.A., Jamir, Y., Alfano, J.R., and Collmer, A. (2004) *Pseudomonas syringae* type III secretion system targeting signals and novel effectors studied with a Cya translocation reporter. *J Bacteriol* **186:** 543–555.

Shan, L., Thara, V.K., Martin, G.B., Zhou, J., and Tang, X. (2000) The *Pseudomonas* AvrPto protein is differentially recognized by tomato and tobacco and is localized to the plant plasma membrane. *Plant Cell* **12:** 2323–2337.

Shedge, V., Arrieta-Montiel, M., Christensen, A.C., and Mackenzie, S.A. (2007) Plant mitochondrial recombination surveillance requires unusual RecA and MutS homologs. *Plant Cell* **19:** 1251–1264.

Sory, M.-P., Boland, A., Lambermont, I., and Cornelis, G.R. (1995) Identification of the YopE and YopH domains required for secretion and internalization into the cytosol of macrophages, using the *cyaA* gene fusion approach. *Proc Natl Acad Sci USA* **92:** 11998–12002.

Tao, Y., Xie, Z., Chen, W., Glazebrook, J., Chang, H.S., Han, B., *et al.* (2003) Quantitative nature of *Arabidopsis* responses during compatible and incompatible interactions with the bacterial pathogen *Pseudomonas syringae*. *Plant Cell* **15:** 317–330.

Tsuda, K., Sato, M., Glazebrook, J., Cohen, J.D., and Katagiri, F. (2008) Interplay between MAMP-triggered and SA-mediated defense responses. *Plant J* **53:** 763–775.

Van den Ackerveken, G., Marois, E., and Bonas, U. (1996) Recognition of the bacterial avirulence protein AvrBs3 occurs inside the host plant cell. *Cell* **87:** 1307–1316.

Wei, C.F., Kvitko, B.H., Shimizu, R., Crabill, E., Alfano, J.R., Lin, N.C., *et al.* (2007) A *Pseudomonas syringae* pv. tomato DC3000 mutant lacking the type III effector HopQ1-1 is able to cause disease in the model plant *Nicotiana benthamiana*. *Plant J* **51:** 32–46.

Xiao, Y., and Hutcheson, S.W. (1994) A single promoter sequence recognized by a newly identified alternate sigma factor directs expression of pathogenicity and host range determinants in *Pseudomonas syringae*. *J Bacteriol* **176:** 3089–3091.

Yang, Y., and Gabriel, D.W. (1995) *Xanthomonas* avirulence/pathogenicity gene family encodes functional plant nuclear targeting signals. *Mol Plant-Microbe Interact* **8:** 627–631.

Yang, B., Zhu, W., Johnson, L.B., and White, F.F. (2000) The virulence factor AvrXa7 of *Xanthomonas oryzae* pv. *oryzae* is a type III secretion pathway-dependent nuclear-localized double-stranded DNA-binding protein. *Proc Natl Acad Sci USA* **97:** 9807–9812.

Yuan, J., and He, S.Y. (1996) The *Pseudomonas syringae* Hrp regulation and secretion system controls the production and secretion of multiple extracellular proteins. *J Bacteriol* **178:** 6399–6402.

Zhou, J.M., and Chai, J. (2008) Plant pathogenic bacterial type III effectors subdue host responses. *Curr Opin Microbiol* **11:** 179–185.

Zipfel, C., Robatzek, S., Navarro, L., Oakeley, E.J., Jones, J.D., Felix, G., and Boller, T. (2004) Bacterial disease resistance in *Arabidopsis* through flagellin perception. *Nature* **428:** 764–767.

Supporting information

Additional Supporting Information may be found in the online version of this article:

Fig. S1. Protein alignment of HopG1 homologues. (*Pto*) *Pseudomonas syringae* pv. *tomato* str. DC3000, NP_794468; (*Pph*) *P. syringae* pv. *phaseolicola* str. 1448 A, YP_273053; (*Rso*) *Ralstonia solanacearum* str. GMI1000, CAD17474; (*Xac*) *Xanthomonas axonopodis* pv. *citri*, ABB84189; (*Xcc*) *X. campestris* pv. *campestris* str. ATCC 33913, NP_638946; (*Aac*) *Acidovorax avenae* ssp. *citrulli* str. AAC00-1, YP_968658 and (*Ret*) *Rhizobium etli* str. CFN 42, YP_471706. Protein sequence data were obtained from NCBI (http://www.ncbi.nlm.nih.gov) and aligned using Clustal W software (http://www.ebi.ac.uk/Tools/clustalw2). Alignment image was created using boxshade 3.21 (http://www.ch.embnet.org/software/BOX_form.html). Conserved putative cyclophilin binding motif (GxLP) is marked with a bar above the conserved sequence.

Fig. S2. A DC3000 *hopG1* mutant is not significantly reduced in its ability to multiply in *Arabidopsis* compared with wild-type DC3000. Wild-type *A. thaliana* Col-0 were spray-inoculated with 1×10^8 cells ml^{-1} of DC3000 or the DC3000 *hopG1* mutant (UNL124) and bacteria were enumerated at 0, 3 and 4 days after inoculation. No significant difference in bacterial growth was observed between the two strains. The experiment was repeated twice with similar results and the standard error bars are indicated.

Fig. S3. HopG1–HA is expressed constitutively in transgenic *A. thaliana*. Immunoblot using anti-HA antibodies of total protein extracts of leaf tissue from wild-type *A. thaliana* Col-0 and a representative *A. thaliana* primary transformant constitutively expressing HopG1–HA. Full-length HopG1–HA is marked by an asterisk (*) and numbers indicate protein molecular weight markers.

Fig. S4. A protein from *X. campestris* with high similarity to HopG1 is targeted to plant mitochondria. NP_638946 from *X. campestris* pv.ca*mpestris* C-terminally fused to the green fluorescence protein ($HopG1_{Xcc}$–GFP) and an N-terminal mitochondrial targeting sequence from isovaleryl-CoA-dehydrogenase fused to the red fluorescent protein eqFP611 (MT–RFP) were transiently coexpressed in tobacco by *Agrobacterium*-mediated transformation and imaged using confocal microscopy. $HopG1_{Xcc}$–GFP, MT–RFP and merged images are shown. The yellow fluorescence in the merged image indicates colocalization of $HopG1_{Xcc}$–GFP and MT–RFP. The experiment was repeated twice with similar results.

Please note: Wiley-Blackwell are not responsible for the content or functionality of any supporting materials supplied by the authors. Any queries (other than missing material) should be directed to the corresponding author for the article.